Polymer 51 (2010) 1311–1319

Contents lists available at ScienceDirect

Polymer

journal homepage: www.elsevier.com/locate/polymer

Fabrication of core or shell reversibly photo cross-linked micelles and nanogels from double responsive water-soluble block copolymers

Qiao Jin, Xiangsheng Liu, Gongyan Liu, Jian Ji*

Department of Polymer Science, Key Laboratory of Macromolecule Synthesis and Functionalization of Minster of Education, Zhejiang University, Hangzhou, 310027, China

ARTICLE INFO

Article history:
Received 27 October 2009
Received in revised form
17 December 2009
Accepted 10 January 2010
Available online 18 January 2010

Keywords:
Photo cross-linking
Nanogel
Micelle

ABSTRACT

Poly(butanedioic acid, 1-[3-[(2-methyl-1-oxo-2-propen-1-yl)oxy]propyl] ester)-b-poly(methoxydi(-ethylene glycol) methacrylate-*co*-4-methyl-[7-(methacryloyl)oxyethyloxy] coumarin) (PSPMA-b-P(DEGMMA-*co*-CMA)) block copolymer was synthesized via atom transfer radical polymerization (ATRP). The temperature and pH responsive micellization behaviors of PSPMA-b-P(DEGMMA-*co*-CMA) were investigated to obtain P(DEGMMA-*co*-CMA)-core and PSPMA-core micelles. After the two types of micelles were exposed to 365 nm UV light, core cross-linked (CCL) micelles and shell cross-linked (SCL) micelles were facilely prepared. The photo cross-linking was proved to be reversibly controlled under alternative irradiation of 365 nm and 254 nm UV light. More interestingly, block copolymer nanogels were fabricated by translating the hydrophobic core of the CCL and SCL micelles into hydrophilic via adjusting the temperature and pH. The sizes of the block copolymer nanogels can be facilely controlled by UV light irradiation. The introduction of reversibly photo cross-linkable groups into the double responsive block copolymers provides a novel approach to develop more sophisticated, controllable, and smarter nanocarriers that might have great potentials in biomedical applications.

1. Introduction

In the last decade, double-hydrophilic block copolymers (DHBCs) having environment-responsive characters have attracted considerable interests due to their potential applications as drug and gene nanocarriers, sensors and catalysis [1–6]. DHBCs are fully soluble in water as unimers under certain conditions. Once adjusting the solution conditions, one block of DHBCs became hydrophobic, while the other block still remained hydrophilic. Self-assembly occurs during this procedure and the unimer-to-micelle transition is completely reversible. Most importantly, the addition of organic solvent is avoided during this micelle-formation procedure. When both blocks of DHBCs are stimuli-responsive, they exhibit intriguing "schizophrenic" micellization behavior, self-assembling into two or more types of micelles with invertible structures [2,7–21]. In each case, the individual block can be independently tuned to become either hydrophilic or hydrophobic depending on the presence of the stimulus. After the first "proof-of-concept" example pioneered by Armes' group who polymerized 2-(*N*-morpholino)ethyl methacrylate (MEMA), followed by 2-(diethylamino)ethyl methacrylate (DEA) using group-transfer polymerization (GTP) [7] a lot of "schizophrenic" micelles have been reported. The extraordinary rich phase behaviors in aqueous solution provide great potentials as smarter nanocarriers for different applications.

However, the practical applications of micelles are limited due to their structural instability since the micellar structure can hardly keep stable upon dilution or changes of external conditions. In order to enhance the stability and structural integrity, core cross-linked (CCL) or shell cross-linked (SCL) micelles were then developed.[22–25] The cross-linked micelles will not be dissociated even in very dilute solutions (<CMC) or in non-selective organic solvents. Various cross-linking approaches have been developed to prepare cross-linked micelles, such as condensation reaction [26] click chemistry [27] and polyelectrolyte complexation [28] et al. Among various chemical and physical cross-linking approaches, the photo cross-linking chemistry [29] has significant importance since no cross-linking agents are needed, and no byproducts are formed during the photo cross-linking procedure [30–33]. Furthermore, the micellar characteristic features, such as micellar size and shape, have been proved to be maintained during the photo cross-linking process [34]. The photo cross-linking procedure, especially the cross-linking density, can be easily controlled by tuning the light wavelength or energy. All of those advantages make the photo cross-linking chemistry as a good choice to tune the stability of micelles. It is well known the stability can be a "double-edged

* Corresponding author. Tel./fax: +86 571 87953729.
E-mail address: jijian@zju.edu.cn (J. Ji).

0032-3861/$ – see front matter © 2010 Elsevier Ltd. All rights reserved.
doi:10.1016/j.polymer.2010.01.026

sword" in controlled delivery system. The biocompatible micelles with good stability can provide an ideal vehicle to delivery the functional molecules, such as peptide, protein, DNA, etc. But after the nanocarriers reach the target, a more stable encapsulation of a guest may render their on-site release more difficult. A stimulus was needed to disrupt the micelles and to facilitate the release. Kataoka and co-workers have proved to solve the problem of the conflicting effect via a reversible disulfide cross-linking in their polyion complex micelles, in which the cross-linked micelles can be dissociated by cleaving the disulfide bond by the intracellular reductive glutathione to release the guest molecules [35]. Zhao and co-workers have synthesized novel coumarin-containing amphiphilic diblock copolymers and demonstrated it is possible to reversibly control the cross-linking and de-cross-linking of micelles by using light at two different wavelengths [29,32,36,37].

Herein, we intended to construct core or shell reversibly cross-linked micelles with double responsive behaviors. We synthesized a novel reversibly photo cross-linked double-hydrophilic block copolymer, poly(butanedioic acid, 1-[3-[(2-methyl-1-oxo-2-propen-1-yl)oxy]propyl] ester)-b-poly(methoxydi(ethylene glycol) methacrylate-*co*-4-methyl-[7-(methacryloyl)oxyethyloxy] coumarin) (PSPMA-b-P(DEGMMA-*co*-CMA)), via atom transfer radical polymerization (ATRP). PSPMA is pH responsive. It is hydrophilic in aqueous solution at high pH (>6) and hydrophobic at low pH. PDEGMMA has recently been used as a new type of thermoresponsive polymer with the lower critical solution temperature (LCST) reportedly at 25 °C in water [38,39]. These novel PDEGMMA polymers can potentially find biomedical applications since they are mainly composed of biocompatible oligo(ethylene glycol) segments. CMA has coumarin side group which provides reversibly photo-cross-linking reaction by the photodimerization of coumarin groups under 365 nm UV irradiation ([2πs + 2πs] cycloaddition reaction) and the photo cleavage of the cyclobutane bridges under 254 nm UV irradiation [32]. We investigated the thermo and pH-responsive micellization behaviors of the polymer PSPMA-b-P(DEGMMA-*co*-CMA). Reversibly SCL and CCL micelles were further prepared using UV irradiation strategy. Moreover, by adjustment of the hydrophobic core of SCL and CCL micelles to hydrophilic, reversibly photo cross-linked block copolymer nanogels were prepared (Scheme 1). We hypothesize here that the introduction of reversibly photo cross-linkable groups into double responsive water-soluble block copolymers will provide a novel approach to develop more sophisticated, controllable, and smarter nanocarriers that might have great potentials in biomedical applications.

2. Experimental section

2.1. Materials

Hydroxypropyl methacrylate (HPMA, mixture of hydroxypropyl and hydroxyisopropyl methacrylates, Aldrich) and methoxydi (ethylene glycol) methacrylate (DEGMMA, Aldrich) were passed through a basic alumina column to remove inhibitor and then stored in a refrigerator before use. Succinic anhydride (SA, alfa aesar) 2,2′-bipyridine (bpy, Aldrich), *N*,*N*,*N*′,*N*′,*N*′-pentamethyldiethylenetriamine (PMDETA), ethyl 2-bromoisobutyate (Aldrich) and 7-hydroxy-4-methylcoumarin (Aldrich) were used as received without further purification. 7-(2-Methacryloyloxyethoxy)-4-methylcoumarin monomer (coumarin methacrylate, CMA) was synthesized as described previously [29].

2.2. Synthesis of poly(hydroxypropyl methacrylate) macroinitiator (PHPMA-Br)

In a typical experiment, ethyl 2-bromoisobutyate (30 μL, 0.2 mmol), HPMA monomer (2 g, 14 mmol) and bpy (62.48 mg, 0.2 mmol) were dissolved in 10 mL of methanol in a 25 mL flask under a N_2 atmosphere. The reaction mixture was degassed by three freeze-pump-thaw cycles. Then nitrogen-degassed CuBr (28.8 mg, 0.2 mmol) was then added quickly to start the polymerization. The reaction mixture turned dark brown immediately. After 3 h, the reaction mixture was quenched by exposing the reaction mixture to air, followed by dilution with methanol (100 mL). The methanol was removed under vacuum and tetrahydrofuran (THF) was added. The catalyst was removed by passing the mixture through a neutral alumina column. The solution was then

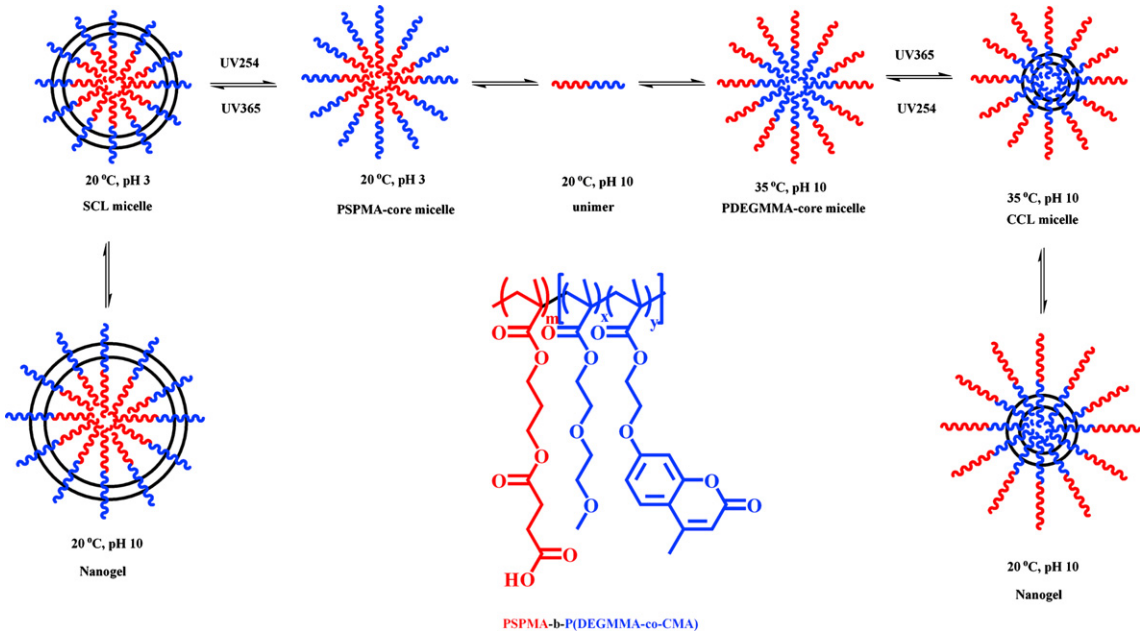

Scheme 1. Schematic illustration of the thermo- and pH-responsive micellization and reversible photo cross-linking of PSPMA-b-P(DEGMMA-*co*-CMA) block copolymer.

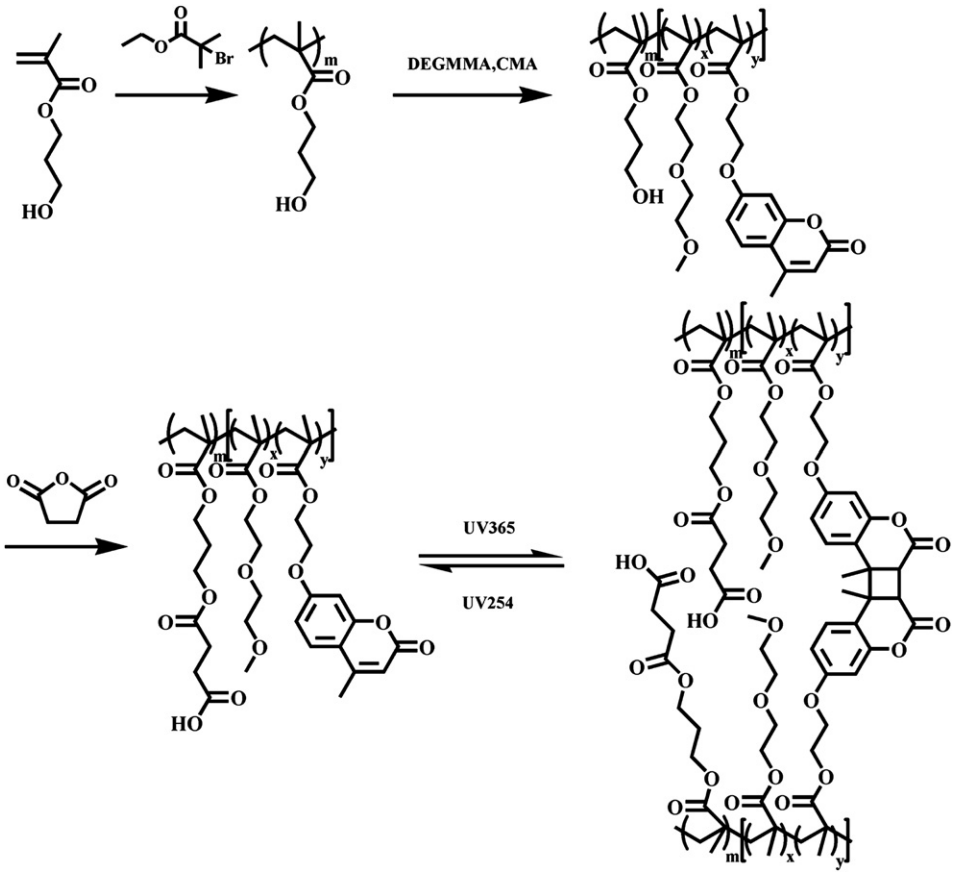

Scheme 2. Schematic illustration of the synthesis and reversibly photo cross-linking of block copolymer PSPMA-b-P(DEGMMA-*co*-CMA).

concentrated and precipitated into deionized water. The moist polymer was dried under vacuum to obtain an off-white solid.

2.3. Synthesis of poly(hydroxypropyl methacrylate)-block-poly(methyl methacrylate-random-coumarin methacrylate) (PHPMA-b-P(DEGMMA-co-CMA))

PHPMA-Br (0.1 mmol), DEGMMA (1.88 g, 10 mmol), CMA (86.5 mg, 0.3 mmol) and PMDETA (21 μL, 0.1 mmol) were dissolved in 10 mL methanol and 2 mL dimethylformamide (DMF) in a 25 mL flask under a N_2 atmosphere. The reaction mixture was degassed by three freeze-pump-thaw cycles. Then nitrogen-degassed CuBr (14.4 mg, 0.1 mmol) was then added quickly to start the polymerization. After 12 h, the reaction mixture was quenched by exposing the reaction mixture to air, followed by dilution with THF. The catalyst was removed by passing the mixture through a neutral alumina column. The solution was then concentrated and precipitated twice in hexane. The block copolymer was dried under vacuum.

Table 1
Polymer compositions, number average molecular weights (Mn), polydispersities (PD) and polymerization degrees (DP) for PHPMA-Br and PHPMA-b-P(DEGMMA-*co*-CMA).

Sample	M_n[a] (GPC)	M_w/M_n[a] (GPC)	DP (theory)	DP[b] (experiment)
$PHPMA_{36}$-Br	6300	1.14	50	36
$PHPMA_{66}$-Br	10400	1.13	100	66
$PHPMA_{36}$-b-P ($DEGMMA_{32}$-*co*-CMA_3)	14100	1.21	50/40/3	36/32/3
$PHPMA_{36}$-b-P ($DEGMMA_{58}$-*co*-CMA_4)	19300	1.27	50/70/4	36/58/4
$PHPMA_{66}$-b-P ($DEGMMA_{86}$-*co*-CMA_6)	29300	1.42	100/100/6	66/86/6

[a] As determined by GPC [calibrated with polystyrene standards].
[b] As determined by ^1H NMR spectroscopy using the ATRP initiator fragment as an end group and relevant signals of both blocks.

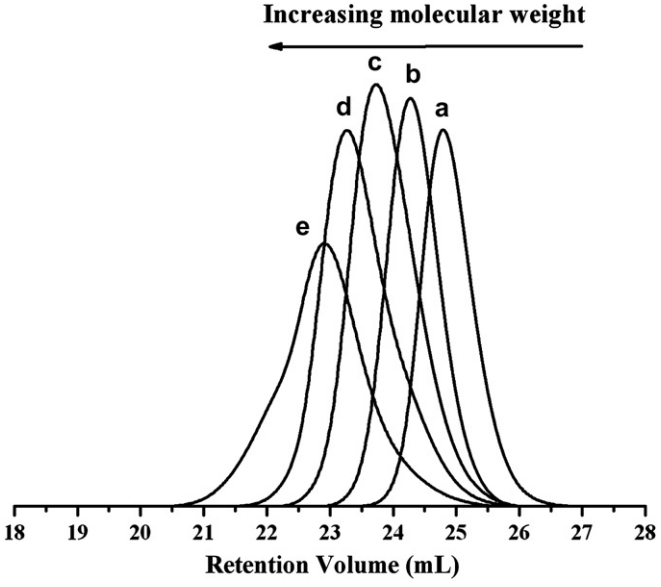

Fig. 1. GPC traces for (a) $PHPMA_{36}$, (b) $PHPMA_{66}$, (c) $PHPMA_{36}$-b-P($DEGMMA_{32}$-*co*-CMA_3), (d) $PHPMA_{36}$-b-P($DEGMMA_{58}$-*co*-CMA_4), (e) $PHPMA_{66}$-b-P($DEGMMA_{86}$-*co*-CMA_6).

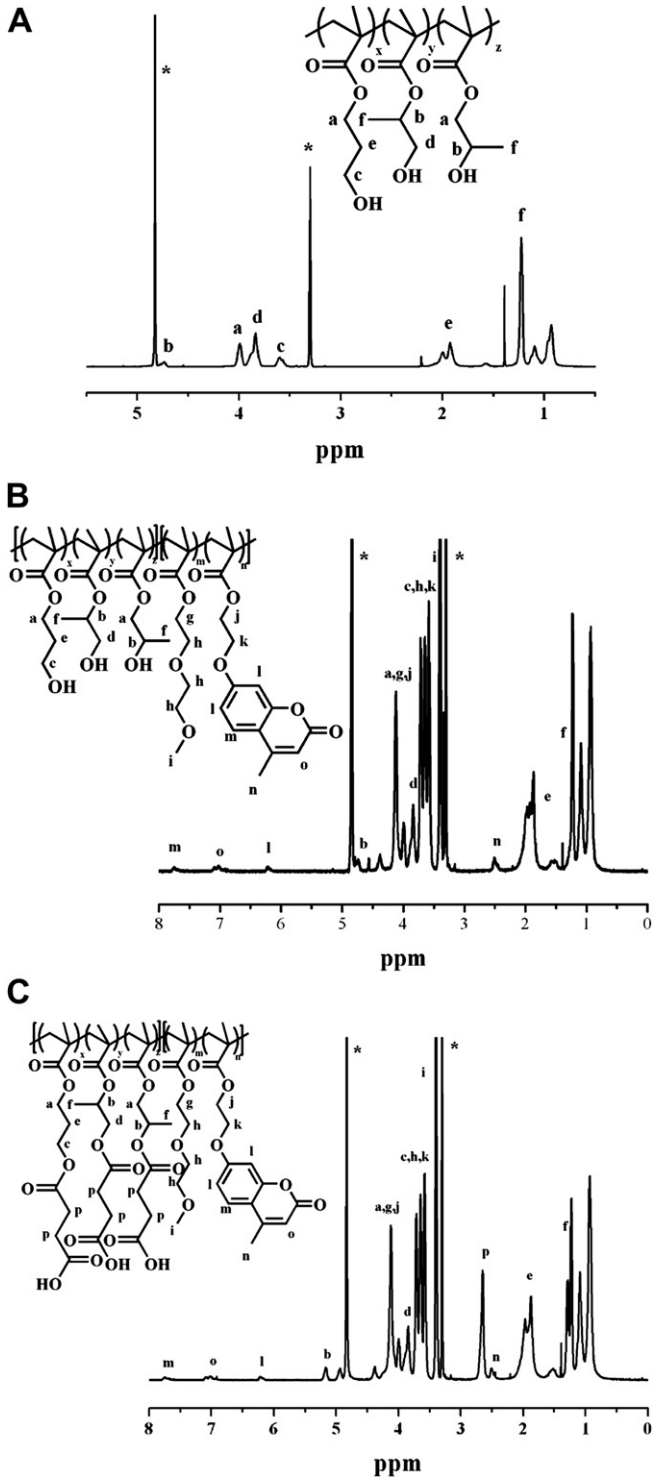

Fig. 2. ^{1}H NMR spectra of (A) $PHPMA_{36}$-Br, (B) $PHPMA_{36}$-b-P($DEGMMA_{58}$-*co*-CMA_4), (C) $PSPMA_{36}$-b-P($DEGMMA_{58}$-*co*-CMA_4) in CD_3OD. *Indicates residual NMR solvent.

2.4. Esterification of PHPMA-b-P(DEGMMA-co-CMA) with succinic anhydride to obtain PSPMA-b-P(DEGMMA-co-CMA)

In a 100 mL round-bottomed flask, PHPMA-b-P(DEGMMA-*co*-CMA) (5 mmol OH residues) was dissolved in anhydrous pyridine (10 mL) at room temperature under nitrogen. Under nitrogen flow, succinic anhydride (1 g, 10 mmol) was added, and the reaction was allowed to proceed at 20 °C for 48 h. Pyridine was partially removed under vacuum, and the copolymer was precipitated into diethyl ether for 3 times. The copolymer was dried under vacuum.

2.5. Micelles preparation

At 20 °C, 2 mg PSPMA-b-P(DEGMMA-*co*-CMA) block copolymer was directly dissolved in 20 mL water by adjusting solution pH to 10 using 1.0 M NaOH under stirring. To obtain P(DEGMMA-*co*-CMA)-core micelles, the solution temperature was increased to 35 °C. The solution was stirred overnight. To obtain PSPMA-core micelles, the solution pH was adjusted to 3 using 1.0 M HCl under stirring at 20 °C. The solution was stirred overnight.

To obtain CCL micelles, 0.1 mg/mL P(DEGMMA-*co*-CMA)-core micelle solution was exposed to 365 nm UV light (200 W) at 35 °C. To obtain SCL micelles, 0.1 mg/mL PSPMA-core micelle solution was exposed to 365 nm UV light (200 W) at 20 °C. In order to get the cross-linked micelles de-cross-linking, cross-linked micellar solution was irradiated under 254 nm UV light (4 W).

2.6. Characterization

2.6.1. Nuclear Magnetic Resonance (NMR) Spectroscopy

All ^{1}H NMR spectra were recorded in D_2O, CD_3OD or $CDCl_3$ using a Bruker DMX500 instrument and scanned in the range 0–15 ppm. Micellization of the diblock copolymers was studied in D_2O using either NaOD or DCl to adjust the solution pH.

2.6.2. Gel permeation chromatography (GPC)

Molecular weights and molecular weight distributions of the homopolymer and copolymer precursors were determined using a GPC setup comprising PL gel 10 μm MIXED-B columns. Calibration was carried out using a series of near-monodisperse polystyrene standards. The GPC eluent was HLPC grade THF, and the flow rate was 1.0 mL min^{-1}. The temperature was set at 40 °C.

2.6.3. Transmission electron microscopy (TEM)

TEM samples were prepared by drying a drop of a dilute aqueous solution of copolymer micelles onto a carbon-coated copper grid. TEM analysis was performed on a JEM-1200EX TEM operating at 200 kV in bright field mode. For the determination of particle size, over 100 particles were counted in multiple pictures from different areas of the TEM grid.

2.6.4. Zeta potential measurements

Zeta potential measurements were carried out on 0.5 mg/mL copolymer solutions using a Malvern Zetasizer3000HSA instrument. The zeta potential (ζ) was calculated from the electrophoretic mobility (u) using the Smoluchowsky relationship, $\zeta = \eta u/\varepsilon$, assuming that $ka >> 1$ (where η is the solution viscosity, ϵ is the dielectric constant of the medium, and k and a are the Debye–Hückel parameters and the particle radius, respectively).

Table 2
Summary of the dynamic light scattering data for PSPMA-b-P(DEGMMA-*co*-CMA) with different polymerization degrees under different conditions.

sample	35 °C, pH 10		20 °C, pH 3		20 °C, pH 10
	$\langle D_h \rangle$/nm	PDI	$\langle D_h \rangle$/nm	PDI	$\langle D_h \rangle$/nm
$PSPMA_{36}$-b-P($DEGMMA_{32}$-*co*-CMA_3)	51.4	0.087	34.8	0.176	6.4
$PSPMA_{36}$-b-P($DEGMMA_{58}$-*co*-CMA_4)	62.2	0.133	33.0	0.217	6.8
$PSPMA_{66}$-b-P($DEGMMA_{86}$-*co*-CMA_6)	80.6	0.205	46.5	0.194	8.4

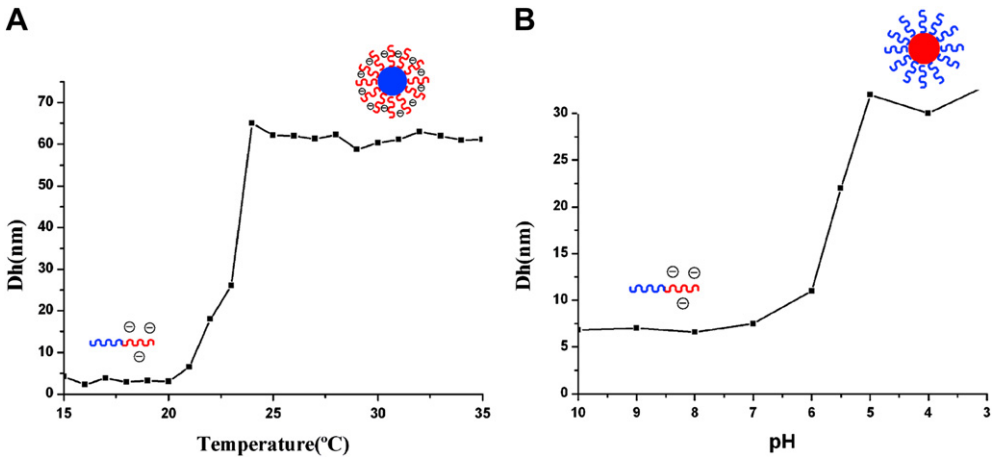

Fig. 3. (A) Temperature-induced micellization of $PSPMA_{36}$-b-P($DEGMMA_{58}$-*co*-CMA_4) block copolymer at pH 10. (B) pH-induced micellization of $PSPMA_{36}$-b-P($DEGMMA_{58}$-*co*-CMA_4) block copolymer at 20 °C.

2.6.5. UV–vis spectra

UV–vis spectra were carried out with a UV–vis Shimadzu UV-2505 spectrometer. Spectra were collected within a range of 300–600 nm.

2.6.6. Laser light scattering (LLS)

A modified commercial light scattering spectrometer (ALV/SP-125) equipped with an ALV-5000 multi-τ digital time correlator and an ADLAS DPY425 II solidstate laser (output power = 400 mW at $\lambda = 532$ nm) was used. In dynamic light scattering (DLS), the line-width distribution $G(\Gamma)$ can be calculated from the Laplace reversion of intensity-intensity time correlation function $G^{(2)}(q,t)$. The reversion was carried out by the CONTIN program. In Static Light Scattering (SLS), the angular dependence of the excess absolute time-averaged scattered intensity of a very dilute dispersion, i.e., the Rayleigh ratio Rvv (q), can lead to the weight averaged molar mass Mw, the second virial coefficient A2, and the z-averaged root-mean square radius of gyration $<Rg^2>_z^{1/2}$, where q is the scattering vector. All the micelle solutions were measured directly without further dilution, and the solutions were cleaned using a 0.45 μm Millipore filter before measurements. All data were averaged over three measurements.

3. Results and discussion

3.1. Synthesis of PSPMA-b-P(DEGMMA-co-CMA)

The synthesis of the PSPMA-b-P(DEGMMA-*co*-CMA) diblock copolymer consists of three consecutive steps. PHPMA-Br was first synthesized via ATRP using ethyl 2-bromoisobutyate as initiator. Then PHPMA-b-P(DEGMMA-*co*-CMA) was synthesized through ATRP using PHPMA-Br as macro-initiator. Finally, PHPMA-b-P(DEGMMA-*co*-CMA) was esterified with succinic anhydride to obtain PSPMA-b-P(DEGMMA-*co*-CMA). The detailed synthesis route was illustrated in Scheme 2.

The successful synthesis of block copolymers PSPMA-b-P(DEGMMA-*co*-CMA) was characterized by GPC and ^{1}H NMR. The number-average molecular weight (M_n) and the polydispersities (PD) of PHPMA-Br and PHPMA-b-P(DEGMMA-*co*-CMA) were determined by GPC using THF as eluent and summarized in Table 1. The GPC chromatograms of PHPMA-Br and PHPMA-b-P(DEGMMA-*co*-CMA) with different targeted DP were given in Fig. 1. As GPC indicated, the resulting polymers had relatively low polydispersity. Typical ^{1}H NMR spectra of each step in the synthesis was shown in Fig. 2, recorded in CD_3OD with the relevant signals labeled. HPMA monomer we used was the mixture of hydroxypropyl and hydroxyisopropyl methacrylates. We can see the characteristic peaks of hydroxypropyl methacrylate (δ3.51–3.65, 3.94–4.06) and hydroxyisopropyl methacrylate (δ 3.79–3.94, 4.69–4.79) in Fig. 2A. Actually, PHPMA-Br was the random copolymer of hydroxypropyl methacrylate and hydroxyisopropyl methacrylate. Fig. 2B showed the ^{1}H NMR spectra of PHPMA-b-P(DEGMMA-*co*-CMA). Both signals ascribed to PHPMA and P(DEGMMA-*co*-CMA) blocks could be observed. For the esterification of PHPMA, 2 equiv of succinic anhydride per OH residue was used with pyridine as basic catalyst [40]. As judged by ^{1}H NMR in CD_3OD, the characteristic PSPMA signal at δ 2.57-2.80 (-OOC-CH_2-CH_2-COO-) was observed in Fig. 2C but was not visible in Fig. 2B. Furthermore, almost all the hydroxy groups in PHPMA were esterified to carboxyl groups judged by ^{1}H NMR. By comparing the well-defined peak integrals of the HPMA, DEGMMA and CMA blocks with that of the ATRP initiator fragment (δ1.37–1.40), the degrees of polymerization, DP, of the HPMA, DEGMMA, and CMA blocks were calculated respectively (Table 1).

3.2. Thermo- and pH-responsive micellization of PSPMA-b-P(DEGMMA-co-CMA)

The combination of thermo-responsive PDEGMMA and pH-responsive PSPMA in a block copolymer leads to a system that responds to both temperature and pH. PDEGMMA can exhibit reversible solubility in water as the temperature changes due to its LCST phase behavior. The solubility of PSPMA in water depends on the pH of the medium. The lower the pH the more carboxylate

Table 3
Structural parameters of P(DEGMMA-*co*-CMA)-core micelles and PSPMA-core micelles formed by $PSPMA_{36}$-b-P($DEGMMA_{58}$-*co*-CMA_4) diblock copolymers under different conditions.

micelle parameters	unimers 20 °C, pH 10	P(DEGMMA-*co*-CMA)-core micelles 35 °C, pH 10	PSPMA-core micelles 20 °C, pH 3
$M_{w,micelles}$[a]	2.43×10^4	4.16×10^6	3.57×10^5
$\langle R_g \rangle$/nm		24.8	
$\langle R_h \rangle$/nm	3.4	31.1	16.5
$\langle R_g \rangle / \langle R_h \rangle$		0.802	
$N_{aggregation}$[b]	1–2	171	15
$\langle \rho \rangle$/(g/cm^3)[c]	/	0.053	0.032
$\mu_2/\langle \Gamma \rangle^2$ [d]	/	0.133	0.217

[a] Average weight of each aggregate.
[b] Average number of the polymer chains inside each aggregate.
[c] The average density of the aggregates, calculated based on $M_{w,micelles}$ and $\langle R_h \rangle$.
[d] The polydispersity index of the size distribution.

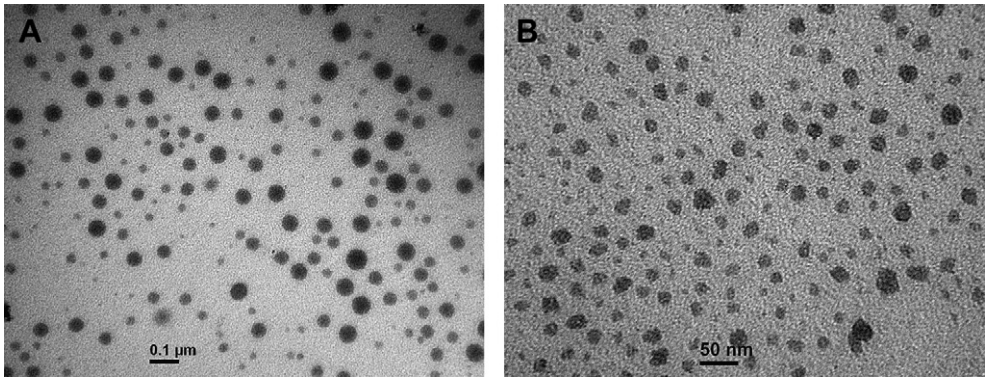

Fig. 4. TEM imagines of $PSPMA_{36}$-b-P(DEGMMA$_{58}$-co-CMA_4) aqueous solution (A) P(DEGMMA-*co*-CMA)-core micelles at 35 °C and pH 10, (B) PSPMA-core micelles at 20 °C and pH 3.

groups of PSPMA are protonated and the less soluble PSPMA becomes in aqueous solution. By subtle adjustment of the solution temperature and pH, PSPMA-b-P(DEGMMA-*co*-CMA) might exhibit thermo- and pH-responsive micellization behavior in aqueous solution. Different sizes of micelles were formed after the change of solution temperature and pH in Table 2. $PSPMA_{36}$-b-P(DEGMMA$_{58}$-*co*-CMA_4) was used to explore the double responsive micellization behavior in detail.

$PSPMA_{36}$-b-P(DEGMMA$_{58}$-*co*-CMA_4) block copolymer was directly soluble in alkaline water (pH 10) at 15 °C. The intensity-average hydrodynamic diameter (D_h) was only 4.8 nm at 15 °C, indicating that the block copolymer was molecularly dissolved in water at pH 10. Upon heating, the D_h started to increase dramatically at ~21 °C, indicating that P(DEGMMA-*co*-CMA) block was getting hydrophobic above its LCST (Fig. 3A). The D_h increased to 62 nm and stabilized out above 25 °C. This suggested thermo-induced micellization. The hydrophobic P(DEGMMA-*co*-CMA) block formed the inner core of the micelles. In addition, the ζ potential of the micellar solution was −50.09 mV at 35 °C and pH 10. It showed that the outer shell of the micelles was ionized PSPMA in this situation.

We further investigated the pH induced micellization of $PSPMA_{36}$-b-P(DEGMMA$_{58}$-*co*-CMA_4) block copolymer. Starting from the unimer state of $PSPMA_{36}$-b-P(DEGMMA$_{58}$-*co*-CMA_4) in aqueous solution at pH 10 and 20 °C, PSPMA-core micelles can also be fabricated via pH changes (Fig. 3B). After 1.0 M HCl was added to adjust the solution pH to acid, ionized carboxylate groups of PSPMA was protonated. PSPMA block became hydrophobic when pH was lower than 5. The D_h increased dramatically from 6.8 nm to 33 nm after the pH was decreased from 10 to 3. The hydrophobic PSPMA block formed the inner core of the micelles. Furthermore, the ζ potential of the micellar solution was 4.58 mV at 20 °C and pH 3. It showed that the outer shell of the micelles was neutral P(DEGMMA-*co*-CMA) block in this situation.

The solution behavior of $PSPMA_{36}$-b-P(DEGMMA$_{58}$-*co*-CMA_4) block copolymer at different temperature and pH was also investigated by dynamic and static light scattering (Table 3). Dynamic light scattering (DLS) showed that P(DEGMMA-*co*-CMA)-core micelles with a $\langle R_h \rangle$ of 31.1 nm were formed at 35 °C and pH 10. At 20 °C and pH 3, PSPMA-core micelles with a $\langle R_h \rangle$ of 16.5 nm were formed. Static light scattering (SLS) studies for the P(DEGMMA-*co*-CMA)-core (35 °C, pH 10) and PSPMA-core (20 °C, pH 3) micelles yielded weight-average micelle masses ($M_{w,micelles}$) of approximately 4.16×10^6 and 3.57×10^5 g mol^{-1}, respectively. On the basis of the weight-average molecular weight (M_w) of $PSPMA_{36}$-b-P(DEGMMA$_{58}$-*co*-CMA_4) determined by SLS at 20 °C and pH 10, the micelle aggregation numbers (N_{agg}) were estimated to be 171 and 15 for the P(DEGMMA-*co*-CMA)-core and PSPMA-core micelles, respectively. Using the equation $\langle \rho \rangle = M_w/(4/3\pi N_a \langle R_h \rangle^3)$, the micelle densities, $\langle \rho \rangle$, of the P(DEGMMA-*co*-CMA)-core and PSPMA -core

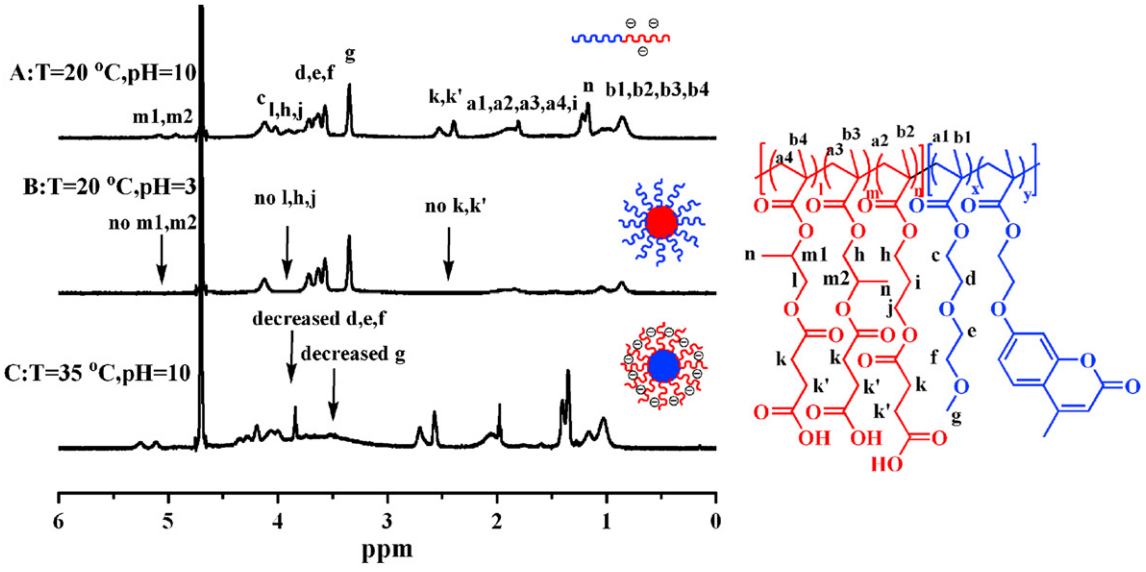

Fig. 5. ^{1}H NMR spectra of $PSPMA_{36}$-b-P(DEGMMA$_{58}$-*co*-CMA_4) in D_2O at (A) 20 °C and pH 10, (B) 20 °C and pH 3, (C) 35 °C and pH 10.

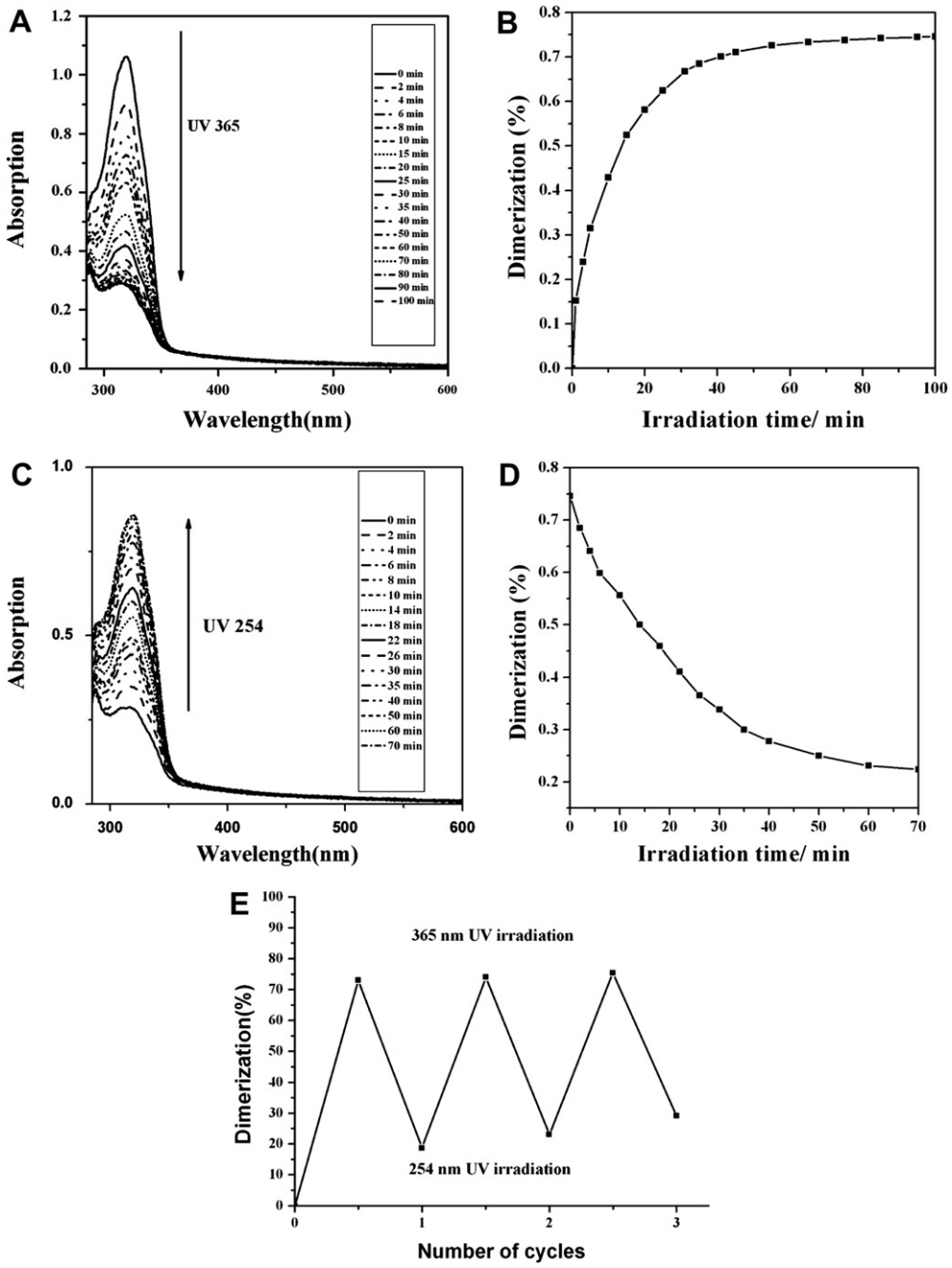

Fig. 6. UV-vis spectra of $PSPMA_{36}$-b-P($DEGMMA_{58}$-*co*-CMA_4) micellar solution at 35 °C and pH 10: (A) under 365 nm UV irradiation, (B) changes of the dimerization degree under 365nm UV irradiation, (C) under subsequent 254 nm UV irradiation, (D) changes of the dimerization degree under 254nm UV irradiation, (E) changes in the photodimerization degree with the solution subjected to alternating irradiations at two wavelengths for 1 h.

micelles were estimated to be 0.053 and 0.032 g cm^{-3}, respectively. Thus the P(DEGMMA-*co*-CMA)-core micelles were somewhat more compact. The large difference in $M_{w,micelles}$, N_{agg} and $\langle\rho\rangle$ showed that P(DEGMMA-*co*-CMA)-core and PSPMA -core micelles were two different types of micellar aggregates. The $\langle R_g\rangle/\langle R_h\rangle$ value of P(DEGMMA-*co*-CMA)-core micelles was 0.802, which was very close to the typical spherical micelles ($\sim$0.775).[41] Unfortunately, the $\langle R_g\rangle$ value of the PSPMA-core micelles was very close to the lower limit of around 10 nm for SLS, which prevented the calculation of a reliable 'R_g'/'R_h' value. TEM images of P(DEGMMA-*co*-CMA)-core (35 °C, pH 10) and PSPMA-core (20 °C, pH 3) micelles revealed the presence of presumably spherical morphologies. The mean number-average diameters were about 46.4 ± 7.2 nm and 24.5 ± 5.1 nm for P(DEGMMA-*co*-CMA)-core and PSPMA-core micelles, respectively (Fig. 4). Taking into account both the degree of hydration and polydispersity effects, the mean diameter determined by TEM compared reasonably well to the average hydrodynamic diameter.

In order to get the direct spectroscopic evidence of the double responsive micellization behavior, Fig. 5 showed the ^{1}H NMR spectra recorded for $PSPMA_{36}$-b-P($DEGMMA_{58}$-*co*-CMA_4) in D_2O at different temperatures and pH values. Because of the hydrophobicity and very low content of CMA units, the CMA signals in D_2O were not visible in the ^{1}H NMR spectra. At 20 °C and pH 10, the PSPMA and P(DEGMMA-*co*-CMA) blocks were both water-soluble, so the signals due to these two solvated blocks were visible in the

^{1}H NMR spectrum (Fig. 5A). PSPMA$_{36}$-b-P(DEGMMA$_{58}$-*co*-CMA$_4$) block copolymer was molecularly dissolved in water. When the temperature was raised to 35 °C at pH 10, the signals attributed to the P(DEGMMA-*co*-CMA) block were greatly suppressed (Fig. 5C), indicating that the P(DEGMMA-*co*-CMA) block formed the dehydrated, less mobile micellar core. On the other hand, when the pH was decreased from 10 to 3 at 20 °C after the addition of DCl, the PSPMA signals disappeared since the protonated PSPMA block became hydrophobic at this pH value. We could only see the signals of P(DEGMMA-*co*-CMA) block. The block copolymer self-assembled to PSPMA-core micelles.

Based on the results obtained by laser light scattering, ^{1}H NMR and TEM, after adjustment of the solution temperature and pH, P(DEGMMA-*co*-CMA)-core and PSPMA-core micelles were organized.

3.3. Core or shell reversibly photo cross-linked micelles formation

The reversibly photo-induced dimerization of coumarins has been well known since the beginning of the 20th century. Upon UV irradiation at $\lambda > 310$ nm, dimers were formed via the $[2\pi s + 2\pi s]$ cycloaddition formation of cyclobutane rings (Scheme 1).[42] The resulting dimers can also be photo-cleaved by exposure to UV irradiation at $\lambda < 260$ nm. Coumarin has been used to construct reversibly photo cross-linked hydrogels [43], micelles [27] and nanoparticles [44] in recent years.

At 35 °C and pH 10, PSPMA$_{36}$-b-P(DEGMMA$_{58}$-*co*-CMA$_4$) block copolymers can self-assemble to P(DEGMMA-*co*-CMA)-core micelles. The micellar solution was then irradiated with 365 nm UV light. Fig. 6A showed the UV–vis spectral change of the P(DEGMMA-*co*-CMA)-core micellar solution upon irradiation of 365 nm UV light. The characteristic absorption peak of coumarin groups at 320 nm decreasing over irradiation time indicated the occurrence of dimerization and thus the cross-linking of the micelles. The dimerization degree, defined as $(1 - A_t/A_0)$ could be calculated from the spectra (A_0 and A_t were the initial absorbance at 320 nm and the absorbance after an irradiation time t, respectively.). The dimerization degree increased very fast at the beginning and reached a plateau value of ~75% after 60 min (Fig. 6B). The D_h of the CCL micelles was 59.3 nm (PDI = 0.141), which was a little smaller than the D_h before cross-linking (62.2 nm). Considering the low concentration of CMA units in the P(DEGMMA-*co*-CMA) block (6 mol % compared to DEGMMA units), it was reasonable to assume that most photo-induced dimerization occurred between coumarin groups on different polymer chains so that the dimerization degree reflected the cross-linking density. Since the resulting dimer form with cyclobutane ring absorbed light at $\lambda < 260$ nm, the core cross-linked micellar solution was illuminated by 254 nm UV light subsequently. The opposite process, i.e., the UV–vis absorbance at 320 nm started to recover, took place as a result of the reverse photo-cleavage reaction bringing back coumarin side groups, as shown in Fig. 6C and D. These results indicate that for the same polymer micellar solution, it is very easy to regulate the cross-linking density by tuning the irradiation time, the intensity and wavelength of irradiation light. Although the photo-cleavage of coumarin dimmers appeared incomplete, a reversible photo control of the cross-linking density could be achieved as shown in Fig. 6E. The dimerization degree could be switched between 75% and 20% by alternating UV exposure at 365 nm and 254 nm for three cycles.

Similar to CCL micelles, SCL micelles were obtained after the PSPMA-core micellar solution was irradiated with 365 nm UV light. The D_h of the SCL micelles was 28.4 nm (PDI = 0.225), which was a little smaller than the D_h before cross-linking (33 nm). Because of the low micellar concentration (0.1 mg/mL) and relatively low content of CMA units (6 mol% compared to DEGMMA units), intermicellar cross-linking was not observed in our experiment. The cross-linking and de-cross-linking process of the SCL micelles were also proved by UV-*vis* spectra similar to CCL micelles (data not shown). The dimerization degree could be easily regulated between 70% and 20% by alternating UV exposure at 365 nm and 254 nm (Fig. 7).

3.4. Reversibly photo cross-linked block copolymer nanogels formation

The successful cross-linking of micelles was also proved by the formation of nanogels. As we know, at 35 °C and pH 10, PSPMA$_{36}$-b-P(DEGMMA$_{58}$-*co*-CMA$_4$) block copolymers can self-assemble to P(DEGMMA-*co*-CMA)-core micelles. If the solution temperature was decreased to 20 °C before cross-linking, P(DEGMMA-*co*-CMA)-

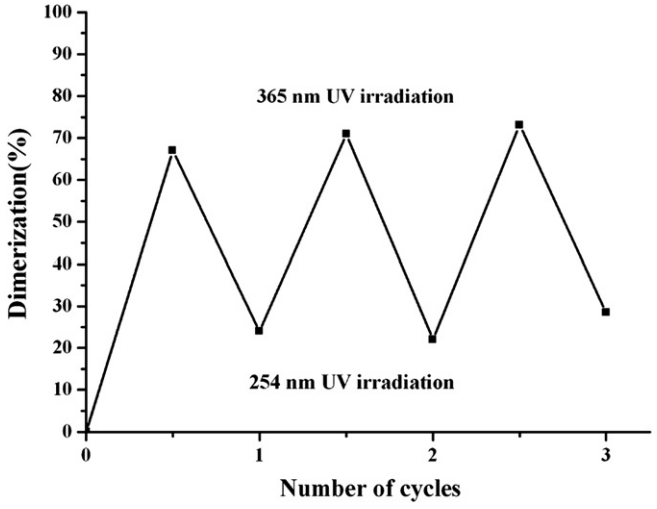

Fig. 7. Reversible change in the dimerization degree of SCL PSPMA$_{36}$-b-P(DEGMMA$_{58}$-*co*-CMA$_4$) micelles at 20 °C and pH 3 upon alternating UV illumination at 365 nm for dimerization (1 h exposure) and at 254 nm for cleavage (1 h).

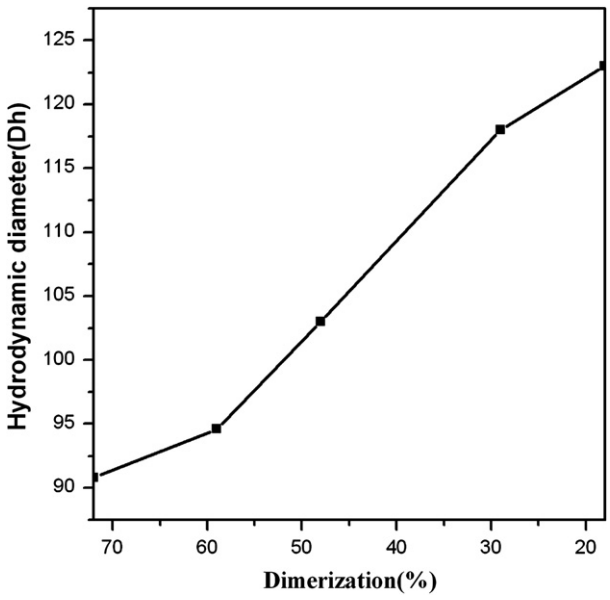

Fig. 8. Dependence of the average hydrodynamic diameter (D_h) on the dimerization degree of the nanogels obtained after the core of CCL P(DEGMMA-*co*-CMA)-core micelles became hydrophilic.

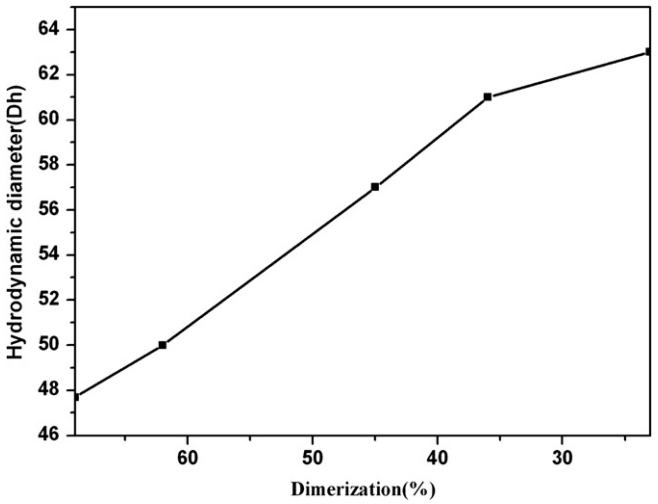

Fig. 9. Dependence of the average hydrodynamic diameter (D_h) on the dimerization degree of the nanogels obtained after the core of SCL PSPMA-core micelles became hydrophilic.

core micelles would disassemble to unimers. On the other hand, if the solution temperature was decreased to 20 °C after photo cross-linking, the micellar aggregates would not disappear although the hydrophobic core of CCL micelles turned to hydrophilic. The CCL micelles became nanogels since they were nanoparticles of cross-linked water-soluble polymer. The D_h of the nanogels was 90.8 nm, which was much larger than that of CCL micelles (59.3 nm). The increase of the D_h might be ascribed to the hydration and swelling of the hydrophobic core of CCL micelles. The dependence of swelling on cross-linking degree suggested that such nanogels could respond to photo exposure. We further investigated the photo-responsive behavior of the nanogels in aqueous solution. Upon the nanogel with 72% dimerization degree was exposed to 254 nm UV light, the cross-linking degree was reduced gradually after the photo-cleavage of coumarin dimers. The volume of the nanogels increased significantly as the D_h went up from 90.8 nm to 123.2 nm (Fig. 8).

To the SCL micelles, after photo cross-linking at 20 °C and pH 3, the solution pH was carefully adjusted to 10 using 1.0 M NaOH. The block copolymer nanogels formed since the core of the SCL micelles became hydrophilic. The D_h of the nanogels was 47.4 nm, which was much larger than that of the SCL micelles (33 nm). We also investigated the photo-responsive behavior of the nanogels in aqueous solution. After the nanogels were irradiated with 254 nm UV light, which induced the photo-cleavage of coumarin dimers, the D_h of the nanogels increased from 47.4 nm to 62.8 nm (Fig. 9). These results clearly showed the photo-induced volume increase of the nanogels was based on the pH 10, 35 n of nanogels. ent micelles were not observed in our experiment. photo-controllable cross-linking density.

4. Conclusions

In summary, ATRP was successfully used to prepare reversibly photo cross-linked thermo- and pH-responsive block copolymer with narrow molecular weight distribution. The PSPMA-b-P(DEGMMA-*co*-CMA) diblock copolymer was well characterized by GPC and ^{1}H NMR. PSPMA-b-P(DEGMMA-*co*-CMA) block copolymer can self-assemble into P(DEGMMA-*co*-CMA)-core micelles at alkaline pH and elevated temperature and PSPMA-core micelles at acid pH and descended temperature. CCL and SCL micelles based on PSPMA-b-P(DEGMMA-*co*-CMA) were prepared by the cross-linking of P(DEGMMA-*co*-CMA) block using photo cross-linking strategy. The photo cross-linking was reversible. The photodimerization of CMA units at 365 nm UV irradiation can result in inter-chain cross-linking, while the cleavage of cyclobutane at 254 nm UV irradiation led to de-cross-linking. The cross-linking density can be facilely controlled by tuning the light wavelength and irradiation time. By adjustment of the hydrophobic core of SCL and CCL micelles to hydrophilic, reversibly photo cross-linked block copolymer nanogels were prepared. This smart multi-stimuli responsive system could lead to more sophisticated, controllable, and smarter nanocarriers that might have great potentials in biomedical applications.

Acknowledgements

Financial support from the Natural Science Foundation of China (NSFC –20774082, 50830106), Programs Foundation of Ministry of Education of China (No. 20070335024), Science Foundation of Chinese University, Open Project of State Key Laboratory of Supramolecular Structure and Materials (SKLSSM200911) and Natural Science Foundation of China of Zhejiang Province (Y4080250) is gratefully acknowledged. The authors are much obliged to Prof. Chen (Fudan University) for his kindly assistance in laser light scattering investigation.

References

[1] Andrew BL, Charles LM. Prog Polym Sci 2007;32:283.
[2] Bütün V, Liu S, Weaver JVM, Bories-Azeau X, Cai Y, Armes SP. React Funct Polym 2006;66:157.
[3] Xu J, Liu SY. Soft Matter 2008;4:1745.
[4] Arotcaréna M, Heise B, Ishaya S, Laschewsky A. J Am Chem Soc 2002;124:3787.
[5] Rodriguez-Hernánadez J, Lecommandoux S. J Am Chem Soc 2005;127:2026.
[6] Ge ZS, Liu SY. Macromol Rapid Commun 2009;30:1523.
[7] Bütün V, Billingham NC, Armes SP. J Am Chem Soc 1998;120:11818.
[8] Liu SY, Billingham NC, Armes SP. Angew Chem Int Ed 2001;40:2328.
[9] Liu SY, Armes SP. Angew Chem Int Ed 2002;41:1413.
[10] Liu H, Li C, Liu H, Liu SY. Langmuir 2009;25:4724.
[11] Jiang XZ, Ge ZS, Xu J, Liu H, Liu SY. Biomacromolecules 2007;8:3184.
[12] Jiang XZ, Zhang GY, Narain R, Liu SY. Langmuir 2009;25:2046.
[13] Chang C, Wei H, Feng J, Wang ZC, Wu XJ, Wu DQ, et al. Macromolecules 2009;42:4838–44.
[14] Rao J, Luo Z, Ge Z, Liu H, Liu SY. Biomacromolecules 2007;8:3878.
[15] Bories-Azeau X, Armes SP, Haak HJW. Macromolecules 2004;37:2348.
[16] Armes SP, Liu SY. Langmuir 2003;19:4432.
[17] Roy D, Cambre JN, Sumerlin BS. Chem Commun; 2009:2106.
[18] Bütün V, Top RB, Ufuklar S. Macromolecules 2006;39:1216–25.
[19] Bütün V, Sönmez S, Yarligan S, Taktak FF, Atay A, Bütün S. Polymer 2008;49:4057.
[20] Zeng J, Shi K, Zhang Y, Sun X, Deng L, Guo X, et al. J Colliod Interf Sci 2008;322:654.
[21] Zhao C, Zhuang X, He C, Chen X, Jing X. Macromol Rapid Commun 2008;29:1810.
[22] Tao J, Liu G, Ding J, Yang M. Macromolecules 1997;30:4084.
[23] Zhang J, Jiang X, Zhang Y, Li Y, Liu SY. Macromolecules 2007;40:9125.
[24] Read ES, Armes SP. Chem Commun; 2007:3021.
[25] Fujii S, Cai Y, Weaver JVM, Armes SP. J Am Chem Soc 2005;127:7304.
[26] Bütün V, Billingham NC, Armes SP. J Am Chem Soc 1998;120:12135.
[27] Jiang X, Zhang G, Narain R, Liu SY. Soft Matter 2009;5:1530.
[28] Weaver JVM, Tang Y, Liu SY, Iddon PD, Grigg R, Billingham NC, et al. Angew Chem Int Ed 2004;43:1389.
[29] Jiang J, Qi B, Lepage M, Zhao Y. Macromolecules 2007;40:790.
[30] Jiang X, Luo S, Armes SP, Shi W, Liu SY. Macromolecules 2006;39:5987.
[31] Kim JS, Youk JH. Polymer 2009;50:2204.
[32] He J, Tong X, Zhao Y. Macromolecules 2009;42:4845.
[33] Yusa S, Sugahara M, Endo T, Morishima Y. Langmuir 2009;25:5258.
[34] Chen Y, Tavakley AE, Mathiason TM, Taton TA. J Polym Sci Part A Polym Chem 2006;44:2604.
[35] Kakizawa Y, Harada A, Kataoka K. J Am Chem Soc 1999;121:11247.
[36] Babin J, Lepage M, Zhao Y. Macromolecules 2008;41:1246.
[37] Dahmane S, Lasia A, Zhao Y. Macromol Chem Phys 2008;209:1065.
[38] Jiang X, Zhao B. Macromolecules 2008;41:9366.
[39] Han S, Hagiwara M, Ishizone T. Macromolecules 2003;36:8312.
[40] Bories-Azeau X, Mérian T, Weaver JVM, Armes SP, Haak HJW. Macromolecules 2004;37:8903.
[41] Zhang Q, Ye J, Liu Y, Nie T, Xie D, Song Q, et al. Macromolecules 2008;41:2228.
[42] Trenor SR, Shultz AR, Love BJ, Long TE. Chem Rev 2004;104:3059.
[43] Nagata M, Yamamoto Y. React Funct Polym 2008;68:915.
[44] Jiang X, Wang R, Ren Y, Yin J. Langmuir 2009;25:9629.